Detection of the Tip of Red Giant Branch in NGC 5128

Roberto Soria[3], Jeremy R. Mould[3], Alan M. Watson[2], John S. Gallagher III[2], Gilda E. Ballester[4], Christopher J. Burrows[5], Stefano Casertano[6], John T. Clarke[4], David Crisp[7], Richard E. Griffiths[6], J. Jeff Hester[8], John G. Hoessel[2], Jon A. Holtzman[9], Paul A. Scowen[8], Karl R. Stapelfeldt[7], John T. Trauger[7], and James A. Westphal[10]

DRAFT

Received ; accepted _____

Submitted to

[1]Based on observations with the NASA/ESA Hubble Space Telescope

[2]Department of Astronomy, University of Wisconsin - Madison, 475 N. Charter St., Madison, WI 53706

[3]Mount Stromlo and Siding Spring Observatories, Institute of Advanced Studies, Australian National University, Private Bag, Weston Creek Post Office, ACT 2611, Australia

[4]Department of Atmospheric and Oceanic Sciences, University of Michigan, 2455 Hayward, Ann Arbor, MI 48109

[5]Space Telescope Science Institute, 3700 San Martin Drive, Baltimore, MD 21218

[6]Department of Astronomy, Johns Hopkins University, 3400 N. Charles St., Baltimore, MD 21218

[7]Jet Propulsion Laboratory, 4800 Oak Grove Drive, Mail Stop 179-225, Pasadena, CA 91109

[8]Department of Physics and Astronomy, Arizona State University, Tyler Mall, Tempe, AZ 85287

[9]Lowell Observatory, Mars Hill Road, Flagstaff, AZ 8600

[10]Division of Geological and Planetary Sciences, California Institute of Technology, Pasadena, CA 91125

ABSTRACT

We present a color-magnitude diagram of 11101'(" than 10,000 still's in the halo of the galaxy NGC 5128 (Centaurus A), based on WFPC2 images through the V and I filters. The position of' the red-giant branch stars is compared with the loci of the RGB ill six Well-stll(lic(l globular clusters and in the dwarf elliptical galaxy NGC 185; the tip of the RGB is signalled by an observed turn-up in the luminosity function at $I \simeq 24.1 \pm 0.1$ mag; this yields a distance 1110(111111s $(m - M)_0 = 27.8 \pm 0.2$ for NGC 5128 (a, distance of 3.6 ± 0.2 Mpc), in agreement with previous determinations based on the planetary nebulae luminosity function and 011 the surface-brightness fluctuations technique.

The presence of an intermediate-age stellar population (~ 5 Gyrs) is suggested by the luminosity function of the AGB stars, extending up to $I = 22.6$ mag (for $V - I > 2$) and M_{bol} 5 mag; however, the 11111111)0' of these stars constrains the intermediate-age stellar population in the halo of NGC 5128 to be less than $\sim$ 10% of the total. The color distribution at constant I magnitude, albeit affected by the completeness level of our sample, strongly suggests a mean value of [1''c/1]] > 0.9 dex, possibly similar to the value found in M31, and higher than that observed in NGC 185.

Subject headings: galaxies: stellar populations

1. INTRODUCTION

Understanding the nature of elliptical galaxies is one of the major ripe problems of astrophysics. Baade's surmise that the stellar population of elliptical galaxies was equivalent to the stellar population of the halo of the Milky Way was based upon resolution of the dwarf elliptical galaxies of the Local Group. More recent insights have suggested galaxy mergers as the origin of these pressure supported stellar systems (Toomre 1972, Schweizer 1994). Either way, the characteristics of the stellar population remain the proving ground for theories of the origin of these galaxies.

NGC 5128 is classified 'S0 pec'; its linkage to elliptical galaxies is through its dominant spheroid (Graham 1979); its linkage to the lenticular class is through its striking and gratuitous disk (Quillen et al 1993). Merger scenarios have been explored by Malin, Quinn & Graham (1983). The galaxy's activity provides a laboratory for gas/jet interaction (Sutherland et al 1993). Its proximity makes it a useful testing ground for early type galaxy distance indicators (e.g. Hui *et al.* 1993, de Vaucouleurs *et al.* 1993).

The resolution and sensitivity of WFPC2 on HST provide a unique opportunity to probe the stellar population of this nearest large early type system. We begin the study by examining a halo field some 9 kpc South of the center of the galaxy; the position of our field is illustrated in Fig. ?? (image taken from the STScI Digitized Sky Survey). We find a stellar population which is in a close relation to that seen in the dwarf ellipticals previously examined from the ground (Mould, Kristian & Da Costa 1983, 1984) and to the halo of M31 (Mould & Kristian 1986).

2. OBSERVATIONS AND PHOTOMETRY REDUCTION

Eight CCD images of a 160" x 160" field in the halo of NGC 5128 were obtained on May 30, 1995 with WFPC2: four through the F555W filter (1100, 1100, 500 and 500 s exposures), and the other four through F814W (600, 600, 1300 and 1300 s exposures). A full description of WFPC2 can be found in both Trauger *et al.* (1994) and the instrument handbook (Burrows *et al.* 1994). Bias subtraction, flat fielding and cosmic ray removal were performed according to the prescriptions of Holtzman *et al.* (1995a) and of Peter Stetson (private communication); the two series of four images were then averaged, in order to obtain a single image (divided into 4 chips and rescaled to 1000 s) for each filter. A section of the resulting F814W image from chip 2 in the Wide Field Camera has been printed in Fig. 1 (size: 40" x 40"). We then vignetted the 4 frames and applied a correction to the pixel area accounting for geometric distortion (the pixel area was rescaled to the average one, following Stetson's convention).

A preliminary list, of stars detected in each chip for each filter was compiled using the automatic star-finding algorithm in DAOPHOT; their instrumental magnitudes were determined with the reduction packages ALLSTAR and ALLFRAME (developed by Peter Stetson) which fit a point-spread-function to each star. The matching program DAOMASTER allowed us to discard stars detected in only one color, as well as stars whose position in the F555W image did not match their position in the F814W image to within 0.04". Eventually, some 11,000 stars were retained (563 of them detected in chip 1, 3422 in chip 2, 3273 in chip 3 and 3827 in chip 4). We then chose several (relatively) isolated bright stars in each chip in order to compare the values of the magnitudes estimated by the point-spread-function fitting algorithm in ALLFRAME with those obtained with aperture photometry, using an aperture radius = 0.5", corresponding to 5 pixels in chips 2, 3 and 4 (Wide Field Camera), and to 11 pixels in chip 1 (Planetary Camera); we verified that this calibration is consistent with the values derived by Peter Stetson and John Holtzman (Stetson, private communication). Unfortunately, the lack of bright stars in chip 1 made our calibration rather uncertain for the PC (we estimated an error of a few tenths of a magnitude); therefore, we decided to adopt Stetson's zeropoints for all four chips, for the sake of consistency. We also introduced a linear correction for the Charge Transfer Efficiency problems explained in Holtzman *et al.* (1995b): pixels located in the 800,1100 row were assumed to be 0.04 mag brighter, while the 1500 row was left unchanged. [11]

Finally, the conversion from the WFPC2 flight photometric system to the standard Cousins colors was implemented using the coefficients tabulated in the same paper: F555W is roughly equivalent to V, and F814W to I (see also Burrows *et al.* 1994). In detail, we used the following relations between ALLFRAME psf magnitudes v and i, and the standard magnitudes V and I:

$$\begin{cases} V = v + 2.5\log(t_{\rm exp}) - A - B_V \cdot (V - I) - C_V \cdot (V - I)^2 \\ I = i - 2.5\log(t_{\rm exp}) - A - B_I \cdot (V - I) - C_I \cdot (V - I)^2 \end{cases} \qquad (1)$$

where $B_V = 0.052$, $C_V = 0.027$, $B_I = 0.063$, $C_I = 0.025$, and the values of A for the different filters and chips have been listed in Table 1; A is the sum of DAOPHOT photometric 0(1's('1 (: 25), plus the zeropoint for a given filter (z.p. = 21.724 for V; z.p. = 20.540" for I), plus a gain factor (different for each chip but ~ 0.75), plus the term required to correct the instrumental magnitudes to a 0.5" aperture radius (of order ~ 0.1), plus a rescaling factor $2.5\log 4$ (all pixel values had been divided by four, initially, as explained in Holtzman *et al.* 1995b).

[11] Although this is a standard correction it is unclear whether it is required for data with this illumination level. We regard our magnitudes as uncertain by $^{+0}_{-0.02}$ from this unknown.

3. COMPARISON WITH GLOBULAR CLUSTER GIANT BRANCHES

Fig. 2 and Fig. 3 display the $(I, V-I)$ and the $(V, V-I)$ color-magnitude diagrams of some 10,000 stars in our field. In the $(I, V-I)$ plane it is easy to see that the dominant contribution comes from the red giant branch (RGB) stars (cf. the analogous CMDs for the dwarf elliptical galaxy NGC 185 plotted in Lee *et al.* 1993a). The number density of the RGB stars rises sharply at $I \approx 24$ mag for $V-I \gtrsim 1.5$ mag, which probably defines the tip of the red giant branch. The RGB tip in the C-M diagram represents the locus of the core helium flash for stars with electron-degenerate cores; stars will follow the RGB during their post-main-sequence evolution, up to the TRGB, where we expect to find a discontinuity in the luminosity function. After the helium flash, stars will at first fall onto the horizontal branch, then move up quickly along the asymptotic giant branch (AGB). Distinguishing between red giant stars near the TRGB and asymptotic giant stars may not always be easy, but the timescale for the evolution along the AGB is much shorter than the time spent on the RGB; hence, the number of AGB stars observed is correspondingly lower. AGB stars will give a relevant contribution to the stars lying at least one mag above the RGB tip: some of the points plotted in Fig. 1 and Fig. 2 may simply be misdetections due to the crowding of our field, but we estimate photometric errors cannot account for all of them; we shall briefly discuss these stars in Sec. 4.2.

The solid lines superimposed on the $(I, V-I)$ color-magnitude diagram are the giant branch loci of six well-studied galactic globular clusters spanning various metal abundances (see Table 2). In order to place those curves on a common scale with the NGC 5128 RGB stars, we need to know the reddenings and the distance moduli of both NGC 5128 and the globular clusters; for the latter, the parameters adopted here are those found in Table IX of Da Costa & Armandroff (1990). The reddening for NGC 5128 has been taken from Burstein & Heiles (1984), using the $E(V-I)/E(B-V)$ relation of Dean *et al.* (1978); this gives $E(V-I) = 0.16 \pm 0.02$ mag and $A_I = 0.22 \pm 0.02$ mag. We tentatively adopt a distance modulus $(m-M)_0 = 27.72$ mag using the results discussed in Hui *et al.* (1993); this value is in agreement with both the distance derived from the planetary nebulae luminosity function and the one inferred with the surface brightness fluctuation technique. From inspection of Fig. 2 it appears that with the adopted modulus the tip of the RGB in NGC 5128 has roughly the same luminosity as the TRGB in the globular clusters; in other words the distance of NGC 5128 determined by comparing the luminosity of the RBG tips (see Sec. 4.1) is consistent with the distance derived with the other two (independent) techniques.

The second relevant piece of information which can be inferred from a comparison of the RGBs in NGC 5128 and in the globular clusters is the metallicity distribution. For a given luminosity, metal-rich stars are redder; the relation between color and metallicity is

non-linear, as we shall see in Sec. 5.

Finally, as explained in Sec. 4.3, we evaluated the photometric errors: we found that the estimates calculated by ALLFRAME are not reliable (they tend to underestimate the true ones); therefore we used the standard technique of adding "artificial" stars in our frames, with random but a priori known position and brightness, and we re-ran all the star-finding algorithms on the new images. We then compared the magnitude of each added stars as determined by ALLFRAME with the value given as input. Not all the fake stars could be recovered, and this allowed us to plot lines in both color-magnitudes diagrams signalling the approximate 50% completeness levels (see Fig. 6 and Fig. 7).

4. LUMINOSITY FUNCTION

4.1. The RGB tip

The RGB tip luminosity is a reliable distance indicator because its I magnitude depends very little upon age (see Green *et al.* 1987) and metallicity, at least for abundances equal or less than [Fe/H] = 0.7 dex (see Da Costa & Armandroff 1990 = DA90). [12] From the giant branch loci in the $(M_I, (V-I)_0)$ plane derived by DA90, we adopted an absolute magnitude $M_{I,\ RGB} = -3.98 \pm 0.12$ mag for the tip; hence, the distance modulus of a galaxy or a cluster of stars can be expressed by the simple relation:

$$(m - M)_0 = I_{I\ RGB} - (-3.98) - A_I \qquad (2)$$

In our case, we know that $A_I = 0.22 \pm 0.02$ mag, and we only need to determine the tip of the RGB from the luminosity function (LF). It is possible in some cases to estimate the position of the discontinuity in the luminosity function simply by eye, but for distant galaxies like NGC 5128 large photometric errors tend to smear out the edge; in a more quantitative approach, one can differentiate the luminosity function and associate the tip of the RGB to the point where the first derivative has a maximum (the point of steepest ascent in the LF). The uncertainty in the detection of the edge depends mostly upon the size of the bins

[12] The DA90 giant branches show that for [Fe/H] > 0.7 the giant branch tip is fainter than specified here. This is due to the effects of bolometric correction in cool stars. (Their luminosities are predicted to be similar to or greater than those of less metal-rich stars). These effects do not bias the RGB tip distance indicator provided metal poor stars are in fact present in the stellar population. They simply soften the luminosity function discontinuity.

into which the data can be collected: in our case we can't choose bins smaller than 0.1 mag in the LF owing to the photometric error. A comprehensive analysis of this method with a computer simulation using artificial LFs can be found in Lee *et al.* (1993b) and Madore & Freedman (1995). The solid line in Fig. 4 displays the LF of NGC 5128; only the stars with $V - I > 1.5$ mag have been considered, in order to make the detection of the edge a little easier; the first derivative of the LF is shown in Fig. 5 (solid line). Five-point smoothing was applied to the luminosity function derivative with the first and last points in the "boxcar" given half weight; three-point smoothing produced similar results.

The result we obtained is $I_{\rm TRGB} = 24.1 \pm 0.1$ mag: this gives a true distance modulus $(m - M)_0 = 27.86 \pm 0.16$ mag, in agreement with the modulus determined from the planetary nebulae luminosity function, $(m - M)_0 = 27.73 \pm 0.14$ mag, and with that derived using the surface brightness fluctuation technique, $(m - M)_0 = 27.71 \pm 0.10$ mag (Hui *et al.* 1993). This confirms the most likely distance to the galaxy is 3.7 ± 0.2 Mpc. The value $I_{\rm TRGB} = 24.0 \pm 0.1$ mag is obtained by considering only the stars detected in PC1 (see Fig. ??): they are a small fraction (1/20) of the total number, but PC1 has a better resolution (0.046" per pixel, while it is 0.1" per pixel in the Wide Field Camera); if we assume this value to be more reliable, the modulus will be $(m - M)_0 = 27.76 \pm 0.16$ mag (3.6 ± 0.2 Mpc).

As a test of the method used to detect the discontinuity in the LF at the tip of the RGB we repeated the same analysis on the LF of the dwarf elliptical galaxy NGC 185, for which the distance modulus had been determined with independent techniques (Lee *et al.* 1993a and Lee, private communication). The true distance modulus of NGC 5128 is now given by:

$$(m - M)_{0,\ \rm NGC\ 5128} = (m - M)_{0,\ \rm NGC\ 185} + I_{\rm TRGB,\ NGC\ 5128} - I_{\rm TRGB,\ NGC\ 185} + A_{I,\ \rm NGC\ 185} - A_{I,\ \rm NGC\ 5128}. \quad (3)$$

The relative shift between the tip of the RGB in the two galaxies appears to be $\Delta I_{\rm TRGB} = 3.65 \pm 0.15$ mag, the tip being found at $I = 20.35 \pm 0.10$ mag for NGC 185 (in good agreement with the value of 20.30 chosen by Lee). We then assume $A_{I,\ \rm NGC\ 185} = 0.38$ mag, and adopt for NGC 185 the distance modulus derived from the absolute V magnitudes of 151 RR Lyrae stars (Saha & Hoessel 1990): $(m - M)_{0,\ \rm NGC\ 185} = 24.02 \pm 0.25$ mag; this leads to a distance modulus $(m - M)_{0,\ \rm NGC\ 5128} = 27.8 \pm 0.3$ mag. The first derivative of the LF for NGC 185 is shown in Fig. 5 as a dashed line.

4.2. Stars above the RGB tip

Although the number density of stars falls quickly for magnitudes $I < I_{\rm TRGB}$ as expected, a few stars are still detected at higher luminosities: we found about 150 stars with $I < 23$

mag and about 50 for $I < 22$ mag, as shown in Fig. 11 and in the C-M diagrams of Fig. 2 and Fig. 3. We can think of three possible explanations for these stars:

a) they are simply misdetections of normal red giant branch stars: in a crowded field two or more stars may happen to be overlapping and may be classified as one bright star by ALLFRAME. We tested this possibility by adding to our images some 1,000 artificial stars fainter than $I = 24$ mag and by checking out how many of them were eventually assigned a magnitude lower than $I = 23$ mag by ALLFRAME. We conclude that photometric errors can explain between 30% and 50% of the detections 0.5 mag above the TRGB magnitude limit.

b) they are foreground Galactic stars. Using the star density calculated by Reid (private communication), we estimate that field contamination in our 5.8 square arcmin field can account for up to 20-25 stars with $18 < I < 24$ mag and $0 < (V - I) < 4$; in particular, at most two or three of them are expected to be found with $22 < I < 23.5$ mag and $0 < (V - I) < 4$. Therefore the effect of Galactic contamination can be neglected at these luminosities, while they can probably explain all the stars seen at $I < 22$ mag.

c) we are detecting real NGC 5128 stars not belonging to the red giant branch. The presence of a few bright, intermediate-color stars with $I \gtrsim 23$ mag and $(V - I) \lesssim 1$ is consistent with the stellar distribution in the C-M diagrams of NGC 185; Lee *et al.* (1993a) suggests these are young, Population I stars, but it seems to us their status is not understood. One might compare them with similar bright stars observed in the stellar constellation Shapley III in the LMC (see Reid *et al.* 1987); in fact, stars above the RGB tip in NGC 5128 appear to be generally similar to those in the LMC. But in the absence of HI gas or interstellar material on the South side of the halo of NGC 5128 the analogy seems strained.

In Fig. 6 and Fig. 7 we approximately identified the position on the color-magnitude diagrams of the different classes of stars discussed above.

We can infer something more about the AGB stars in NGC 5128 by plotting an $(M_{\rm bol} - (V - I)_0)$ color-magnitude diagram, as we did in Fig. 8; we adopted a distance modulus $(m - M)_0 = 27.72$ mag, while the bolometric correction to the I magnitude was taken from Da Costa & Armandroff 1990 as:

$$BC_I = 0.881 - 0.243(V - I)_0 = 0.920 - 0.243(V - I). \qquad (4)$$

From this diagram, and from the slope of the bolometric luminosity function plotted in Fig. 9, we see that the AGB extends up to $M_{\rm bol} \sim 5$ mag. A natural explanation of the ~ 300 stars in the range $(-5, 4)$ in $M_{\rm bol}$ is that a very significant fraction of the star formation in NGC 5128 occurred just ~ 5 Gyrs ago. Aaronson & Mould (1985) have shown that LMC clusters of age 5 Gyr reach $M_{\rm bol} = 1.5$ on the AGB. Allowing for the possibility that some

half of the stars in this magnitude range may have been promoted there by confusion, we see that the ratio of these stars to stars at the RGB tip is similar in NGC 5128 to its value in M32 (Freedman 1989, 1992). O'Connell (1980, 1986) has argued convincingly that the age of the dominant stellar population in M32 is 5 Gyr (but see Renzini 1992). (The current event in this galaxy is presumably of much more recent origin). If the elliptical galaxy NGC 5128 formed in a merger, could this have been its approximate date?

We can calculate the number, n, of upper AGB stars expected in a 5 Gyr old population with the aid of

$$bL_V \tag{5}$$

(Renzini & Buzzoni 1984) where L_V is the visual luminosity of the population and t is the lifetime of stars in this interval on the AGB. The luminosity sampled can be estimated from the surface photometry of van den Bergh 1976. Assuming the average surface brightness is $\mu_V = 23.5$ mag/arcsec^2, we obtain $L_V = 7 \times 10^7 L_\odot$ for the area sampled. Adopting $b = 3 \times 10^{-11}$ and $t = 0.7 \times 10^6$ years for the half magnitude between -4 and -4.5 in $M_{\rm bol}$ (Renzini 1978), one predicts 1500 stars. This would constrain a burst of star formation from a merger to add only ~10% to the pre-existing stellar population.

Moreover, we cannot rule out the hypothesis that these upper AGB stars represent a high metallicity tail of the distribution, which in some way, possibly a low mass loss rate, ascend the AGB like a younger population. Stars with $M_{\rm bol} = -5$ are observed in the nuclear bulge of the Milky Way (Terndrup *et al.* 1990), although these stars may themselves be intermediate age (Holtzman *et al.* 1992).

In summary, AGB star counts seem to push the major epoch of star formation in NGC 5128 back earlier than 5 Gyrs ago, although unknown mass loss / metallicity dependences allow a great deal of flexibility to the model maker.

4.3. Completeness

The ADDSTAR task of DAOPHOT proved to be a powerful tool for estimating the completeness of our sample and the photometric error as a function of magnitude. We added 500 stars on each of the WFPC2 chips both in the V and in the I images with random position (but coincident in both filters) and random magnitudes in the range $22.5 < I < 27.5$ mag and $23.5 < V < 28.5$ mag. (it is easy to verify the completeness level is 1 for stars brighter than $I = 22.5$ mag and $V = 23.5$ and is 0 for stars fainter than $I = 27.5$ mag and $V = 28.5$). The new frames containing all the real plus the fake stars were then run through the same routines (DAOPHOT, ALLSTAR, ALLFRAME, DAOMASTER) in

order to produce a new list of stars and respective magnitudes; this was then compared with the original list of artificial stars (from which we subtracted all the stars falling in the vignetted areas of each image). The ratio between the initial and the final number of added stars allowed us to determine the completeness functions at each magnitude, as shown in Fig. 10; we applied these curves when we determined the color (hence also the metallicity) distribution at fixed values of I (see Sec. 5). A limitation of the ADDSTAR task is the fact that stars are created with the same point-spread-function which is then used as a template to detect them; in other words they are probably slightly easier to find than real stars, and the completeness level may be a little overestimated.

The artificial stars experiment also helped us determine the photometric errors in I', I and V I as a function of magnitude; the original magnitudes were compared with the PSF magnitudes derived by ALLFRAME, and the resulting error bars are shown in Fig. 2 and Fig. 3. Systematic errors begin to affect the data near or below the 50% completeness level, where only stars with positive fluctuations in their luminosity are detected. Occasionally, errors larger than 1 mag ()("('lll' due to an overlapping of stars in our crowded field; this explains only in part the large number of stars found above the TRGB; besides, this effect is more evident in the I magnitude, and such misdetected stars are more frequently found atveryred ("0101'S."

5. METALLICITY DISTRIBUTION

The color dispersion in the magnitude below the RGB tip is large and real and is naturally explained by a range in metallicity in this halo sample. At I = 24.4 mag the color dispersion is $\sigma \simeq$ 0.54 mag; the measuring error in color is $\sigma \simeq 0.15$ mag.

The relation between the intrinsic color of the RGB and the metal content of its stars can be approximated by (see Da Costa & Armandroff 1990):

$$[1''('/11] = 15.16 + 17.()(1' \quad I)_{0,-3} \; 4.9[(V\,I)_{0,-3}]^2, \tag{6}$$

where $(V \quad I)_{0,-3}$ is the color of the RGB at M_I = 3, ie 1 mag below the RGB tip. The relation is valid for $-2.2 < [Fe/H] < 0.7$. Alternatively, for the same range of metal abundances we can adopt the relation:

$$[Fe/H] = -12.64 + 12.61(V - I)_{0,-3.5} - 3.33[(V - I)_{0,-3.5}]^2, \tag{7}$$

derived by Lee *et al.* (1993a), where we defined $(V \quad I)_{0,-3.5}$ as the intrinsic color of the RGB half a mag below the tip; this relation is more useful in our case, because of the low level of ("01111 pleteness affecting our data ill I ~25mag.

In Fig. 11 we show horizontal cuts across the RGB at three such magnitudes after correction for completeness. These distribution functions in turn constrain the metallicity distribution function dn/d[Fe/H]. We find that over the range (−1.5, −0.5) in [Fe/H] dn/d[Fe/H] is a rising function, although only for $I = 24.2$ do we have a sample of stars with [Fe/H] > −0.7 and completeness > 50%. We conclude that the mean value of [Fe/H] exceeds −0.9 in this halo field in NGC 5128, conservatively disregarding samples at $I = 24.5$ and 24.8 which require mean values exceeding −0.75, but rely on completeness corrections of a factor of two or more.

We note that Mould & Kristian (1986) using similar techniques found [Fe/H] > −0.6 for their halo field in M31. If the halo metallicity / luminosity relation is a guide (Da Costa & Mould 1988), these relatively high metallicity values may be characteristic of the halos of luminous galaxies with $M_V \simeq -21$.

6. CONCLUSIONS

The main conclusions we can derive from the present work are:

1) the distance modulus for NGC 5128 inferred from the luminosity of the tip of the red-giant branch is in agreement with the values previously determined using the planetary nebulae luminosity function and the surface brightness fluctuation; for NGC 185 it is also in agreement with the distance derived from the luminosity of its RR Lyrae stars. This is a further indication of the reliability of the TRGB method, extensively discussed in Madore & Freedman (1995).

2) we notice the presence of bright stars, blue in $(V - I) = 1$; bright, blue stars have also been observed in the dwarf elliptical NGC 185 by Lee *et al.* (1993a).

3) on the other hand, the observed number of AGB stars in the range $-5 < M_{\rm bol} < -4$ mag (well above the RGB tip) constrains an episode of star formation in consequence of a merger to add less than about 10% to the pre-existing stellar population; the major epoch of star formation was probably earlier than 5 Gyrs ago, although large uncertainties remain in the evolutionary models.

4) finally, the position of the red-giant branch in the C-M diagram implies a mean value of [Fe/H] higher than −0.9 (quite larger than the mean metallicity in NGC 185); relatively high metallicity values have previously been found in a halo field in M31. The crowding of our field (causing large photometric error) and, above all, a completeness level falling below the 50% limit already a 1 mag below the tip of the RGB are the main sources of uncertainty in our analysis.

We are grateful to Daya Rawson and Peter Stetson for contributing their expertise in photometry. JRM and RS thank Gary Da Costa for a critical reading of the manuscript; RS also thanks John Graham for his stimulating remarks and suggestions. This research was carried out by the WFPC2 Investigation Definition Team for JPL and was sponsored by NASA through contract NAS7-1260.

REFERENCES

Aaronson, M. & Mould, J. 1 ApJ, 288, 551

Burstein, D. & Heiles, C. 1984, ApJS, 54, 33

Burrows, C. J. (ed.) 1994, Wide Field and Planetary Camera 2 Instrument Handbook, STScI publication.

Da Costa, G. S. & Armandroff, T. E. 1990, AJ, 00, 162.

de Vaucouleurs, G. 1993 ApJ, 415, 33.

Dean, J. F., Warren, P. R. & Cousins, A. W. J. 978, MNRAS, 183, 569.

Freedman, W. 1989, AJ, 98, 1285.

Freedman, W. 1992, in The Stellar Populations of Galaxies, IAU Symposium 149, eds. B. Barbuy & A. Renzini, p. 169.

Graham, J. 1979, ApJ, 232, 60.

Green, E. M., Demarque, P. & King, C. R. 1987, The Revised Yale Isochrones and Luminosity Functions, Yale University Observatory.

Holtzman, J. A., Faber, S. M., Shaya, E. J., Lauer, T. R., Groth, E. J., Hunter, D. A., Baum, W. A., Ewald, S. P., Hester, J. J., Light, R. M., Lynds, C. R., O'Neil, E. J. & Westphal, J. A. 1992, AJ, 103, 691

Holtzman, J. A. 1995, private communication.

Holtzman, J. A., Hester, J. J., Casertano, S., Trauger, J. T., Watson, A. M. & WFPC 2 IDT 1995a, PASP, 107, 156.

Holtzman, J. A., Burrows, C. J., Casertano, S., Hester, J. J., Trauger, J. T., Watson, A. M. & Worthey, G. 1995b, (in press).

Hui, X., Ford, H. C., Ciardullo, R. & Jacoby, G. H. 1993 ApJ, 414, 463.

Iben, I., Renzini, A. & Schramm, D. N. 1978, Advanced Stages of Stellar Evolution, eds. P. Bouvier & A. Maeder.

Lee, M. G. 1995, private communication

Lee, M. G., Freedman, W. L. & Madore, B. F. 1993a, AJ, 106, 964

Lee, M. G., Freedman, W. L. & Madore, B. F. 1993b, ApJ, 417, 553

Madore, B. F. & Freedman, W. L. 1995, AJ, 109, 1645.

Malin, D., Quinn, P. & Graham, J. 1983, ApJL, 272, L5.

Mould, J., Kristian, J. & Da Costa, G. S. 1983. ApJ, 270, 471.

Mould, J., Kristian, J. & Da Costa, G. S. 1984. ApJ, 278, 575.

Mould, J. & Kristian, J. 1986, Ap. J., 305, 591.

O'Connell, R. 1980, ApJ, 236, 430.

O'Connell, R. 1986, in Stellar Populations, STScI Symposium Series # 1. eds. C. Norman, A. Renzini & M. Tosi, p. 167.

Quillen, A. 1993 ApJ, 412, 550.

Reid, N., Mould, J. & Thompson, I. 1987, ApJ, 323, 433

Reid 1995, private communication.

Renzini, A. 1992, in The Stellar Populations of Galaxies, IAU Symposium 149, eds. B. Barbuy & A. Renzini, p. 325.

Renzini, A. & Buzzoni, A. 1986, in Spectral Evolution of Galaxies, eds. C. Chiosi & A. Renzini (Dordrecht: Reidel).

Saha, A. & Hoessel, J. G. 1990, AJ, 99, 97.

Schweizer, F. 1994, IAU Symposium 164, in press.

Stetson, D. B. 1995, private communication.

Sutherland, R., Bicknell, G. V. & Dopita, M. A. 1993, ApJ, 414, 510.

Terndrup, D., Frogel, J. A. & Whitford, A. E. 1990, ApJ, 357, 453.

Trauger, J. T. & WFPC-2 IDT 1994, ApJL, 435, L3.

van den Bergh, S. 1976, ApJ, 208, 673.

Watson, A. M., Mould, J. R., Gallagher III, J. S. & WFPC-2 IDT 1994, ApJL, 435, L55.

This manuscript was prepared with the AAS LaTeX macros v3.0.

Filter	PC1	WF2	WF3	WF4
V	0.967 ± 0.018	0.958 ± 0.009	0.950 ± 0.009	0.973 ± 0.011
I	1.861 ± 0.017	1.823 ± 0.014	1.842 ± 0.009	1.870 ± 0.013

Table 1: Value of the adopted zeropoint ZP for the different filters and chips.

Cluster	[Fe/H]	$M_{I,\,\mathrm{TRGB}}$
NGC 7078 (M 15)	-2.17	-4.095
NGC 6397	1.91	-3.765
NGC 7089 (M2)	1.58	-4.035
NGC 6752	-1.54	-3.948
NGC 1851	-1.29	-4.02
NGC 104 (47 Tuc)	0.71	-4.039

Table 2: Galactic globular clusters adopted for a comparison with NGC 5128

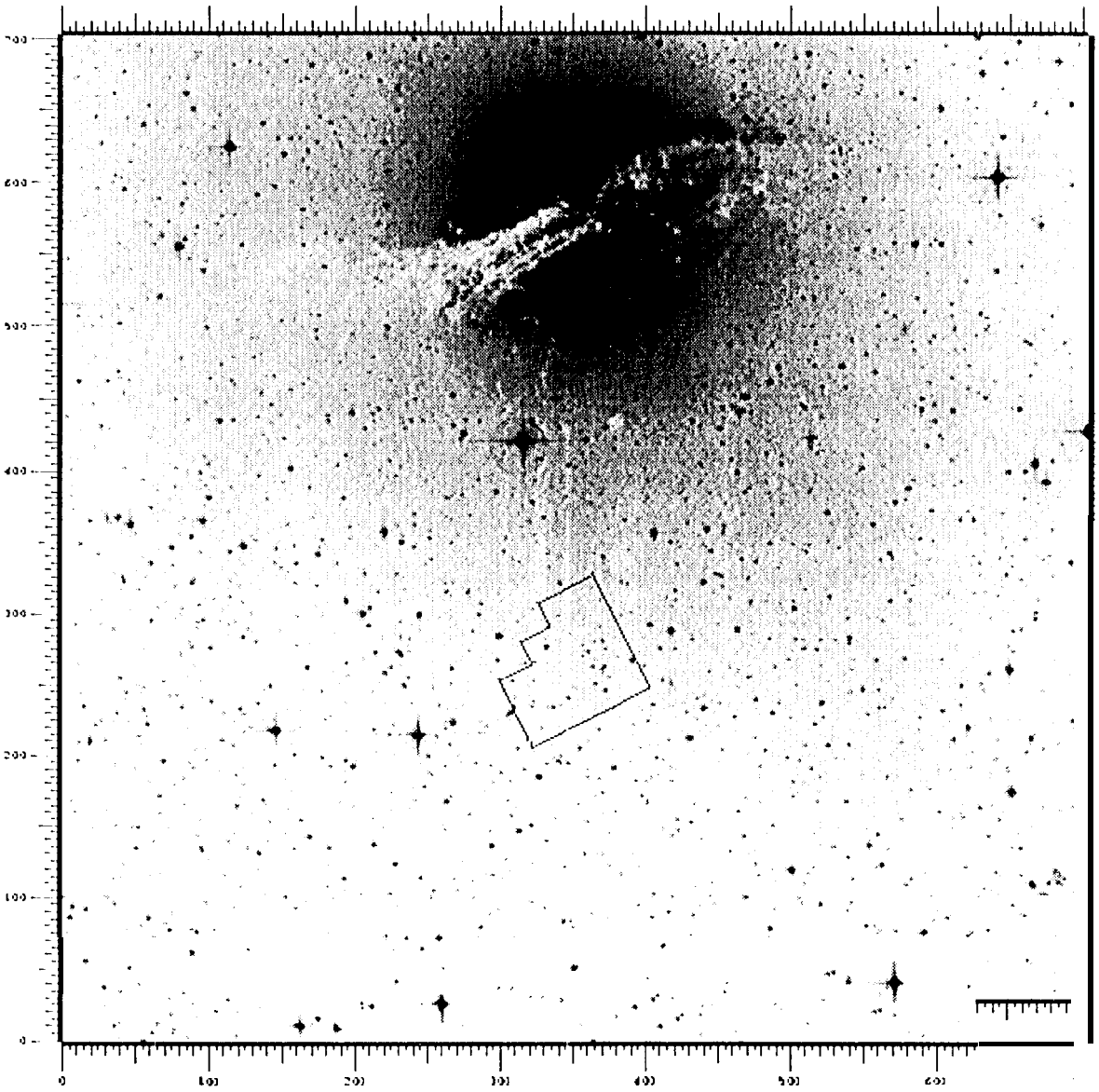

Fig. 1 Position of our field in the halo of NGC 5128; image from the STScI Digitized Sky Survey; size: 20" x 20'.

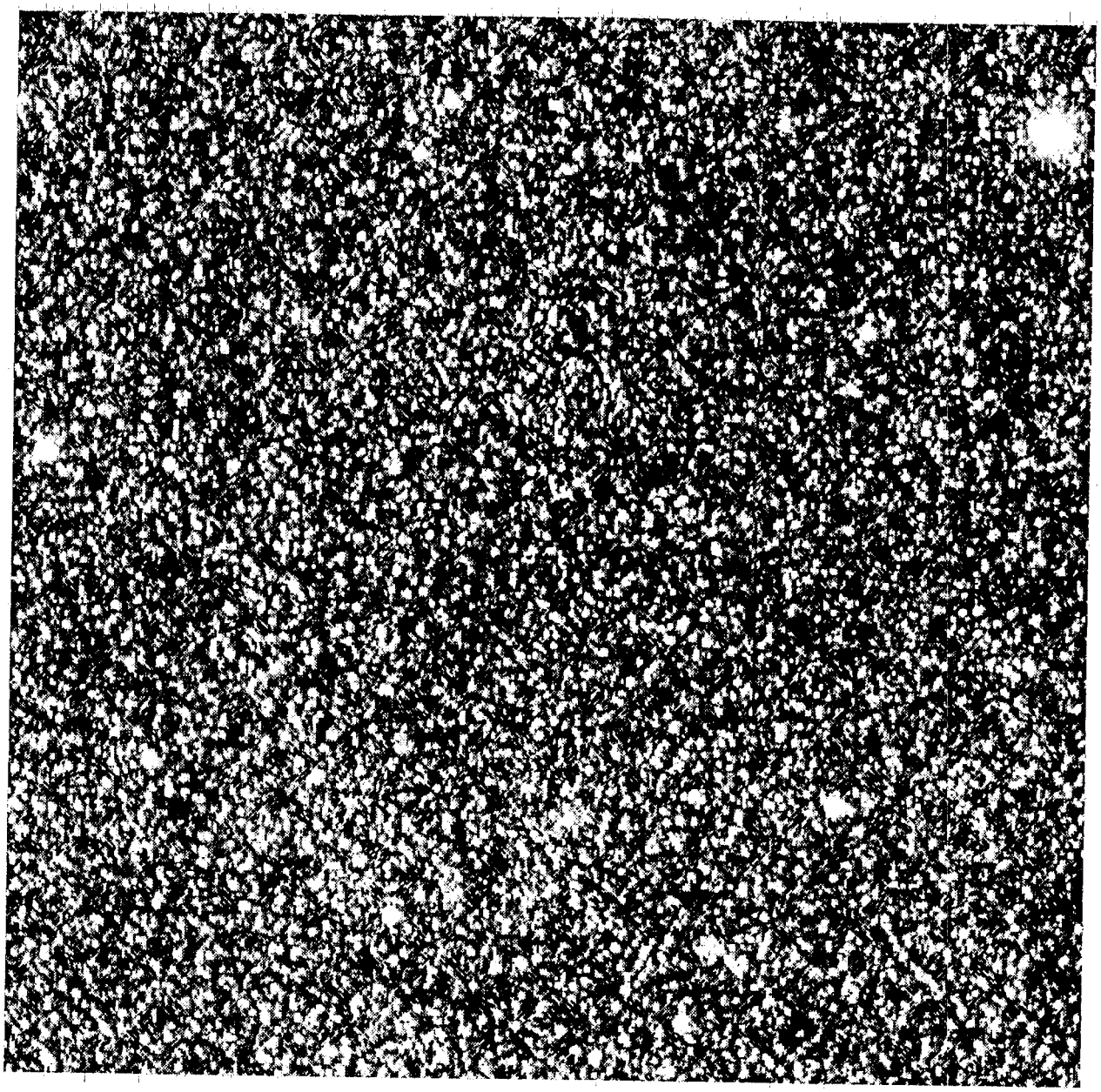

NGC 5128 - Halo

F814W image, chip 2

The original image was 800 by 800 pixels
This is a 400 by 400 pixel subset, with lower left corner at pixel [illegible]
Black corresponds to a data value of 55.0, and white to 100.0
The image file was image2_2
Printed at Sat Sep 23 21:22:49 1995 for roberto by IL ASER Version [illegible]

Fig. 2. Image of a 40" x 40" field in the halo of NGC 5128 taken with WF2 of the WFPC2, through the infrared filter F814W; the image has already been bias- and cosmic ray-subtracted.

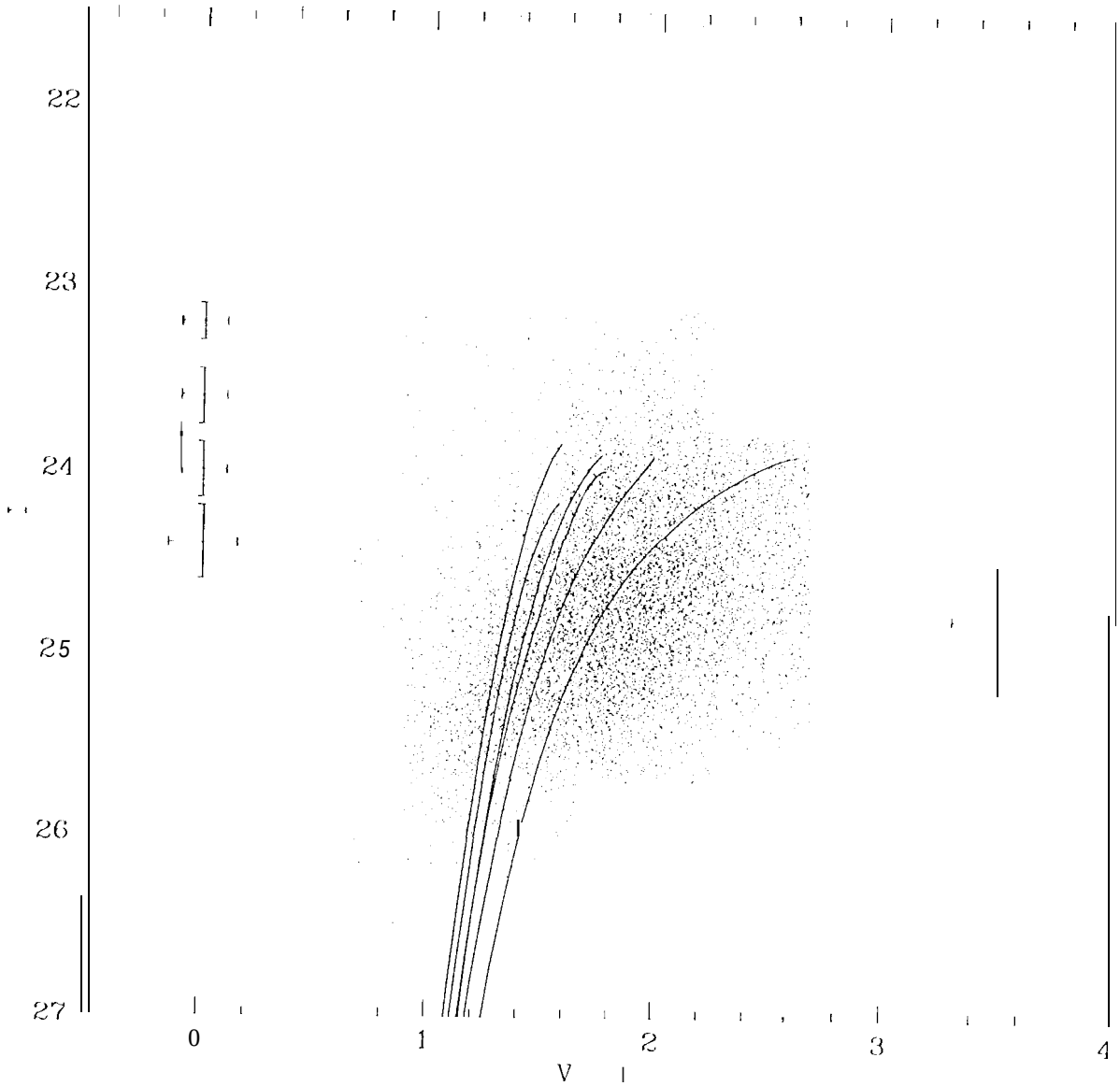

Fig. 3. Color-Magnitude diagram in the $(I, V-I)$ plane for about 10,000 stars in the halo of NGC 5128. The mean photometric error at various magnitudes has been determined by using the ADDSTAR task of DAOPHOT. The solid curves are the loci of the giant branches in six globular clusters studied by Da Costa & Armandroff (1990); from the left to the right, they are M15, NGC 6397, M2, NGC 6752, NGC 1851, 47 Tuc; see the text for the adopted values of reddening and modulus.

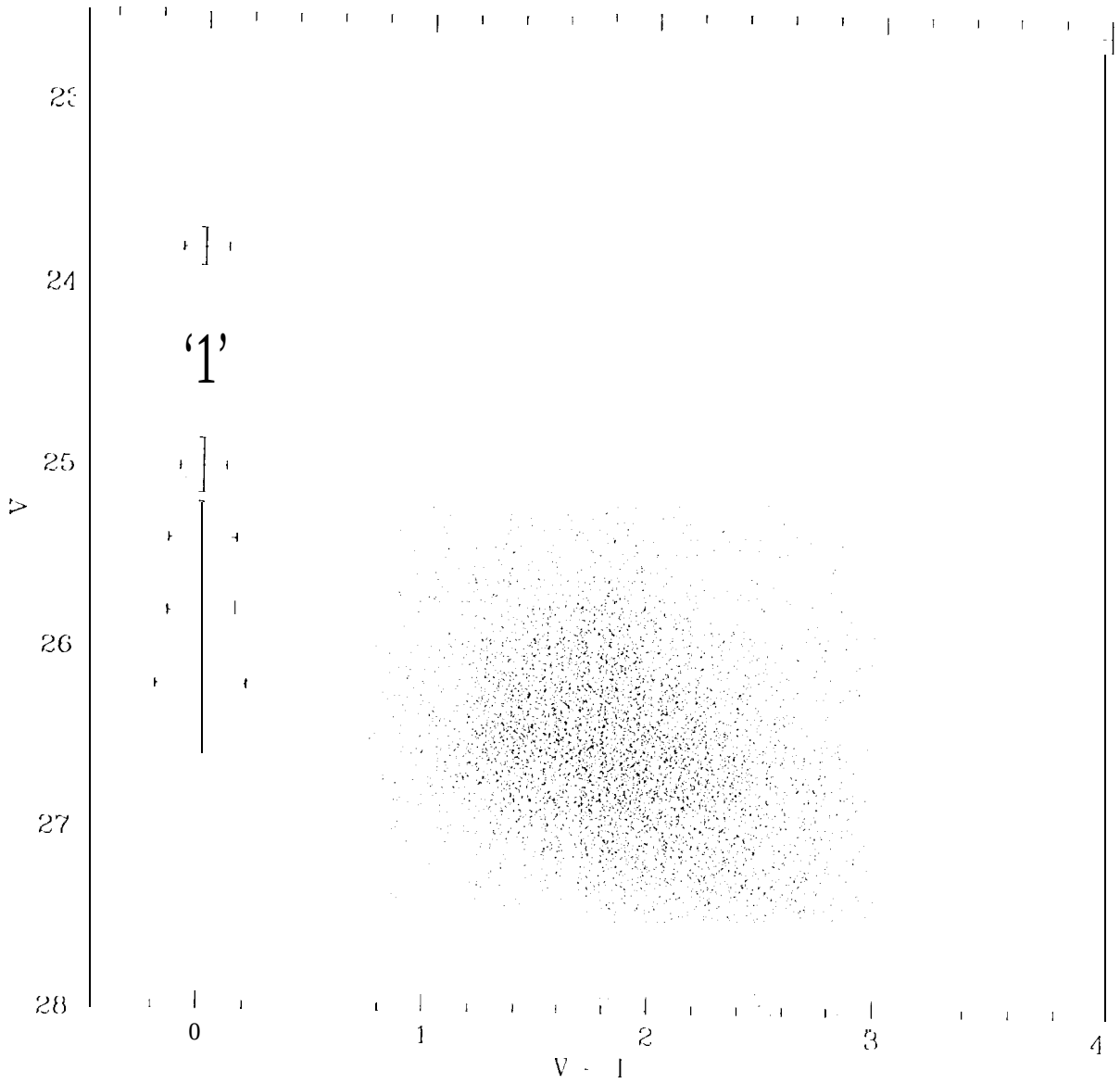

Fig. 4. Color-Magnitude diagram in the $(V, V - I)$ plane for the same stars as in Fig. 2 The photometric error has been determined as before.

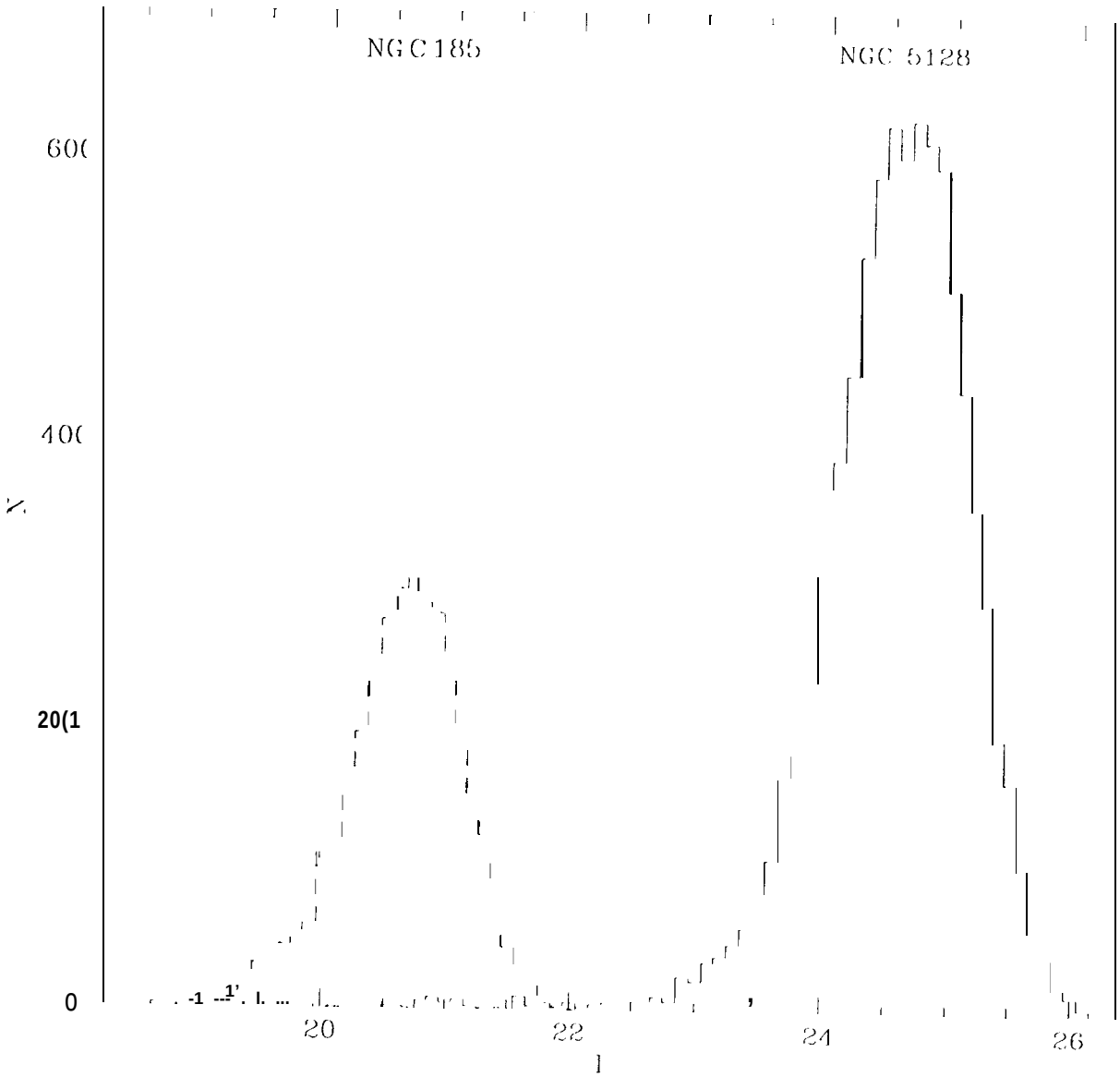

Fig. 5. – Luminosity functions for the RGB stars in NGC 5128 (solid line) and NGC 185 (dashed line); only stars redder than V – I = 1.5 have been considered.

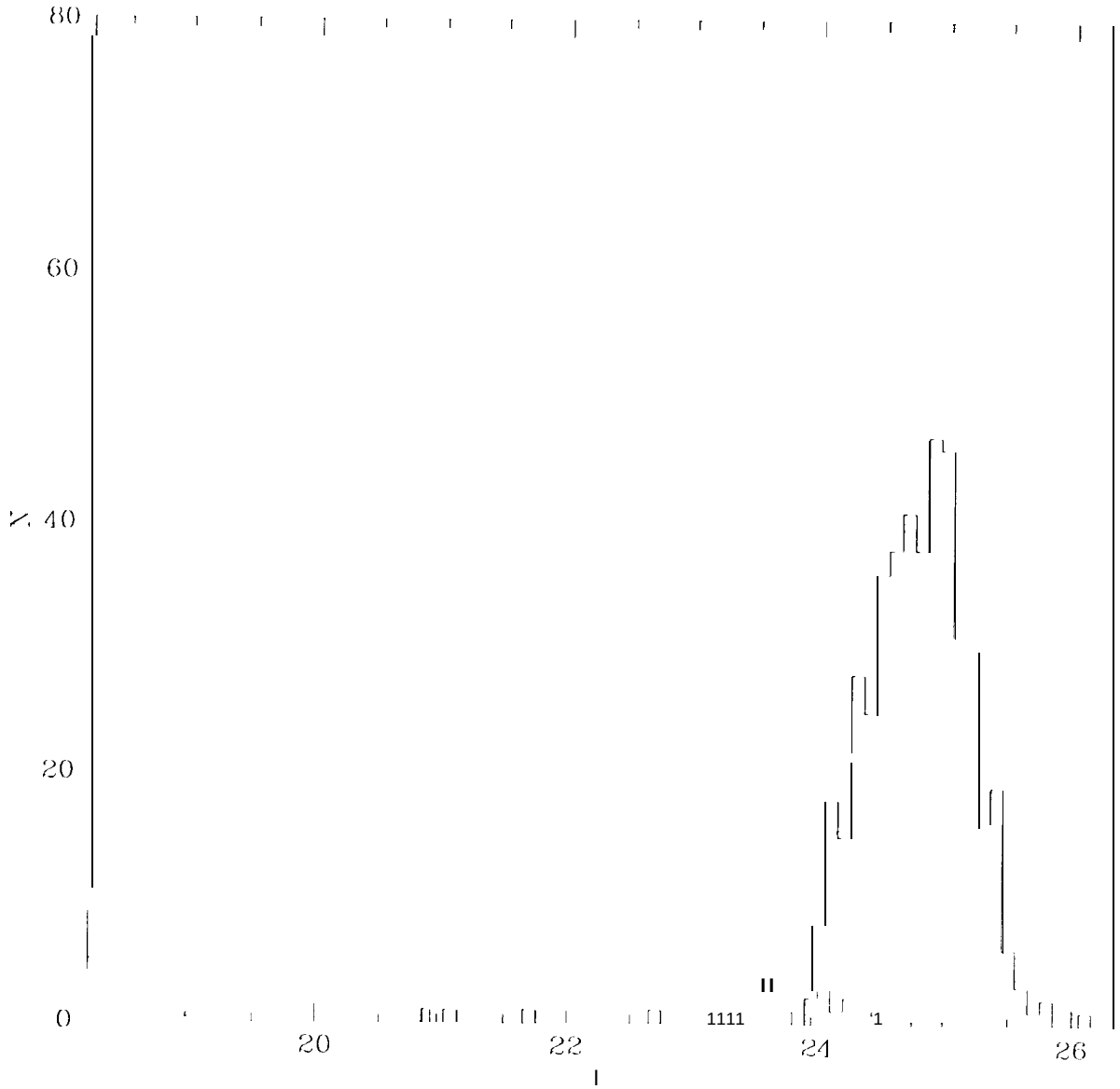

Fig. (i. / Luminosity functions for the RGB stars in NGC 5128 detected in PC 1: only stars l'(, (1(1('! thanV / 1.5 have been consid ered, as before. 1 he turn-up in the LF at I 24.0 I (1.1 mag is moreevident.

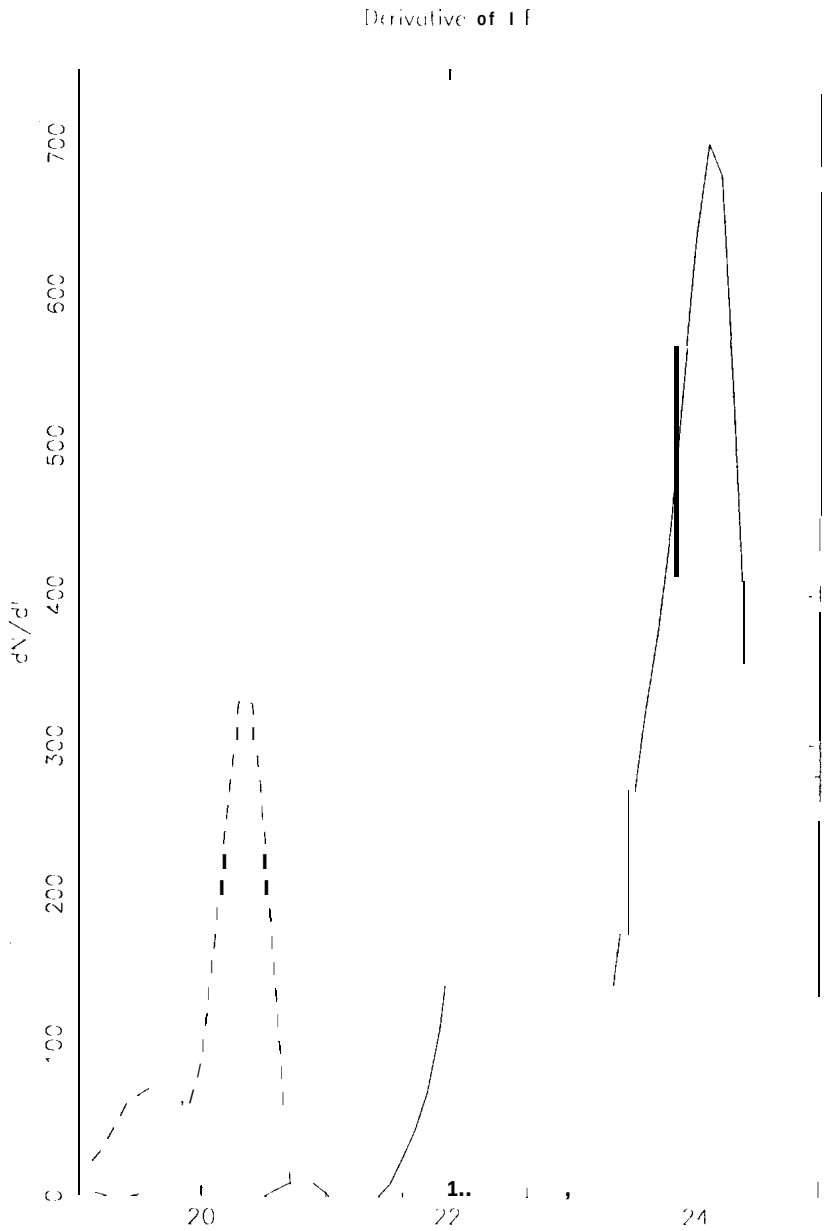

Fig. 7. – First derivative of the I luminosity function in NGC 5128 (solid line) and NGC 185; we can associate the tip of the RGB with the maximum in the LF's first derivative

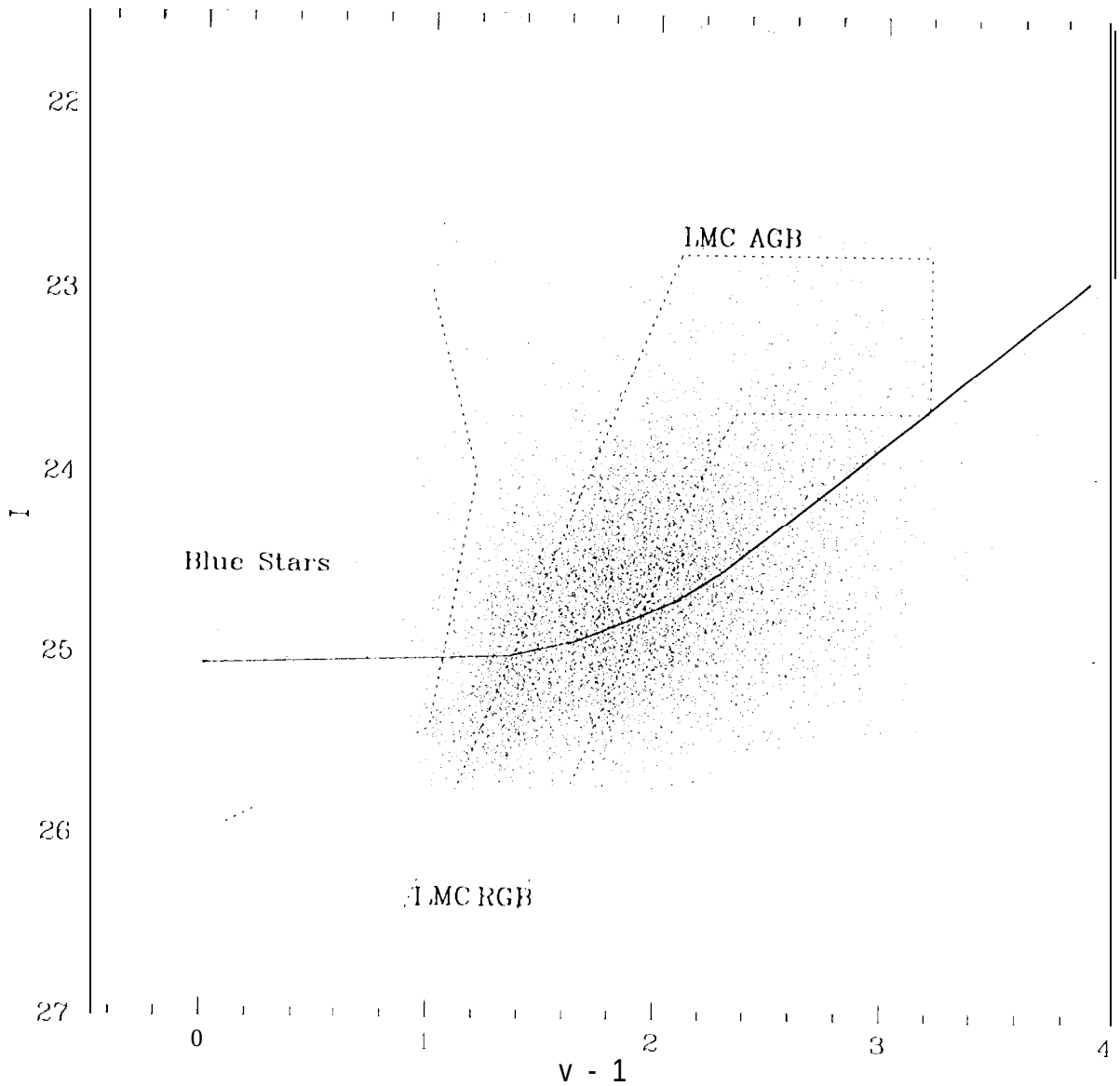

Fig. 8. Color-Magnitude diagram in the (I, 1'- I) plane, with the 50% completeness level indicated by a solid line; the dotted lines defines the approximate locus of the Blue Stars (see text) and the 10('(1S 01" the RGB and AGB stars in the Large Magellanic Cloud field studied by Reid *et al.* (1987).

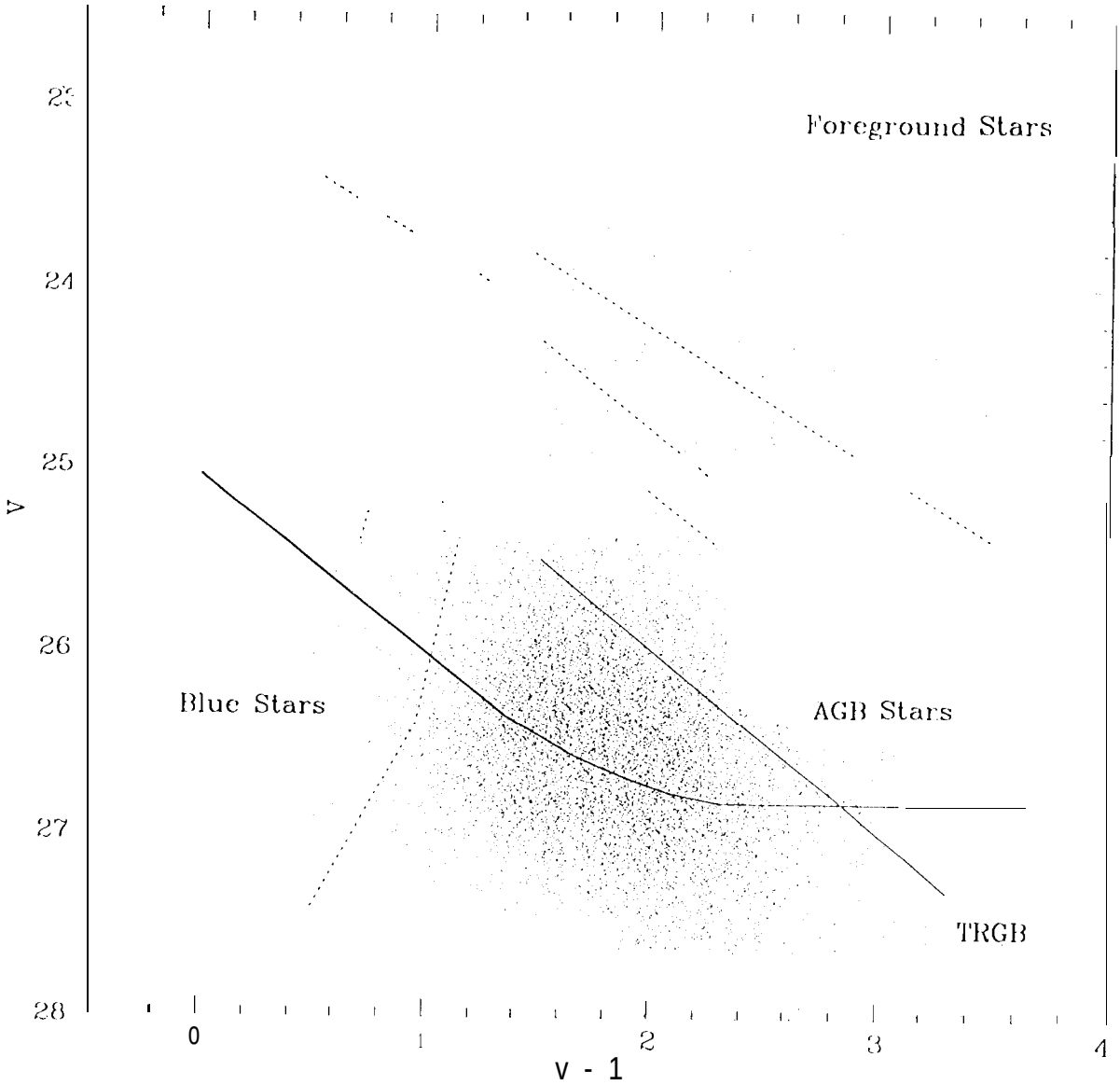

Fig. 9. Color-Magnitude diagram in the $(V, V - I)$ plane; again, we have displayed the loci of the Blue Stars and of the AGB stars; the bright, red stars in the upper right corner are likely to be Galactic foreground stars; the thin, solid line marks the tip of the RGB and the thick line is the 50% completeness level of our sample.

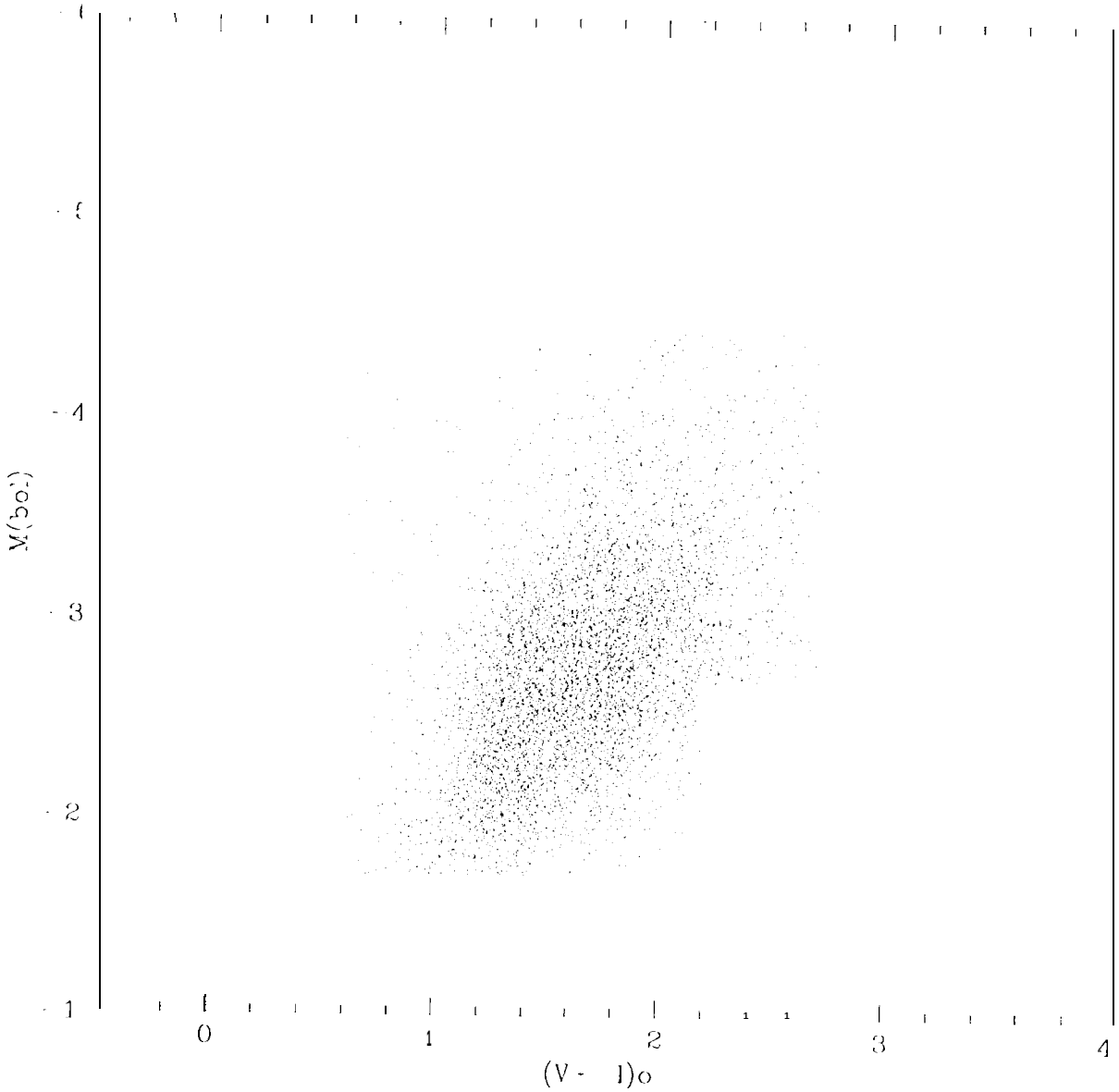

Fig. 0. Color-Magnitude diagram in the $((M_{bol}, (V - I)_o)$ plane for the stars in NGC 5128.

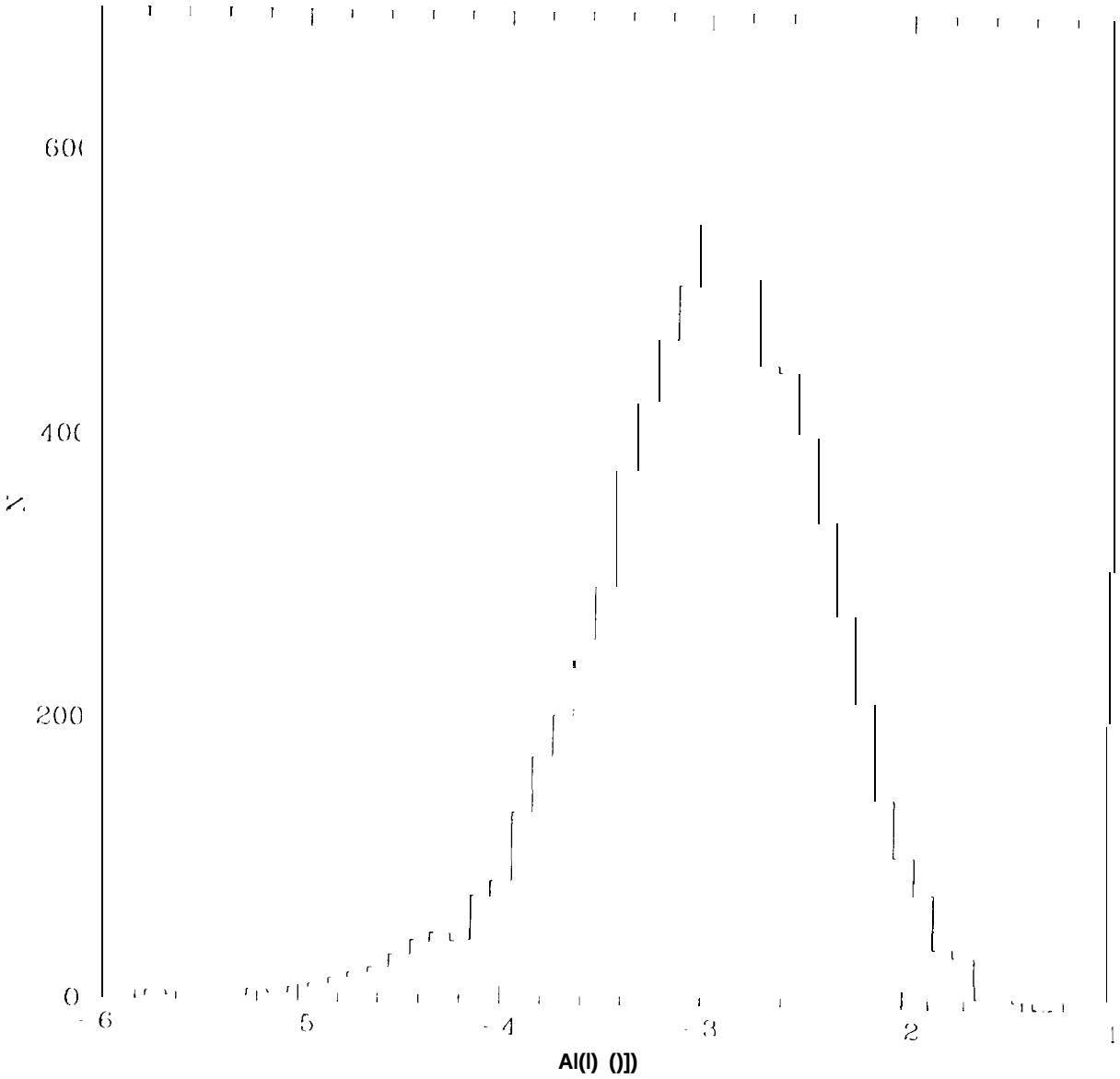

Fig. 11. M_{bol} luminosity function for our field in the halo of NGC 5 28; the brightest AGB stars ('X1(,11(1 up to ,1/,)(), ~ 5.

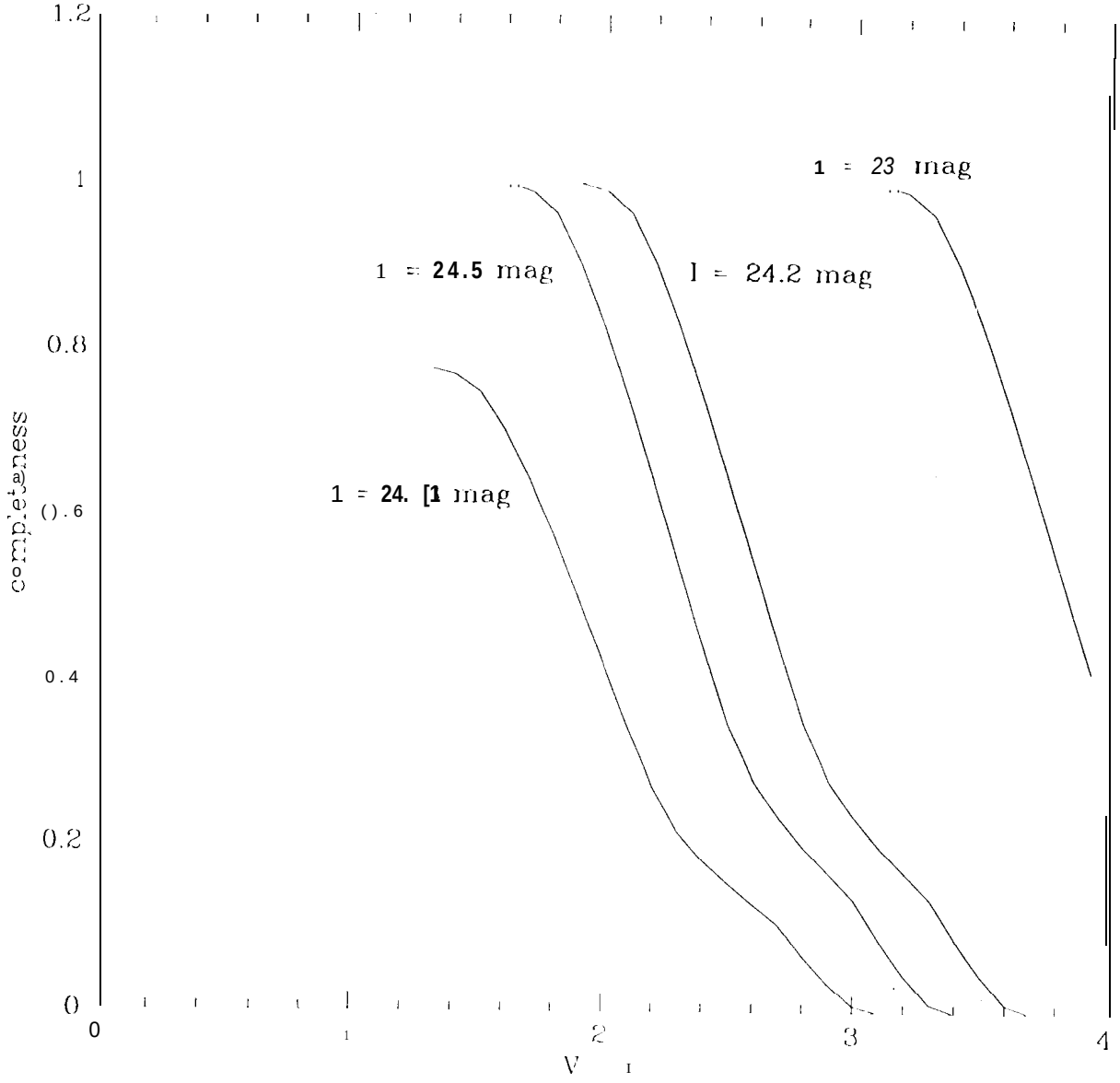

Fig. 12. Completeness level of our sample as a function of $V - I$, for different values of I; the ADDSTAR algorithm was used to determine these curves.

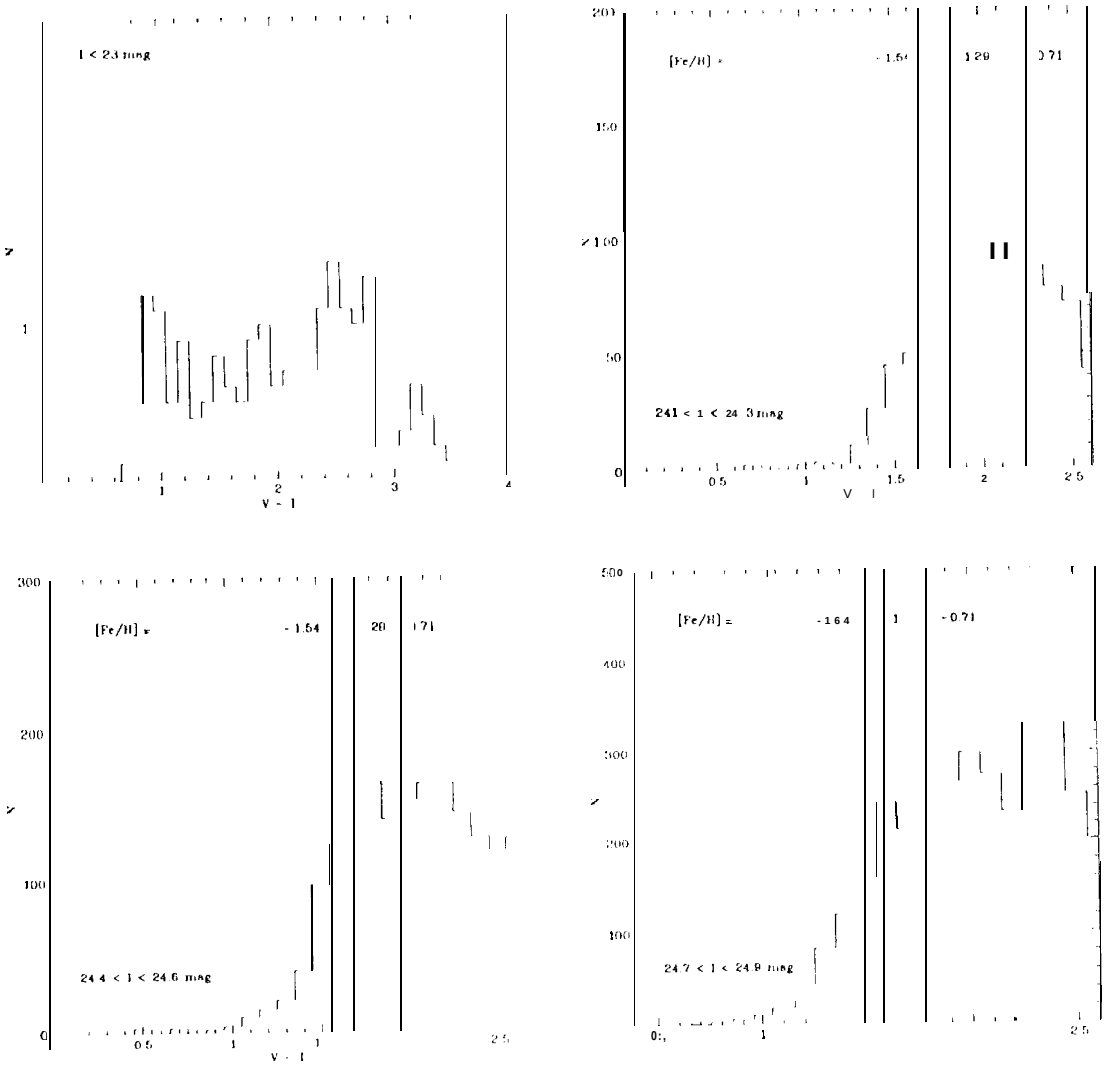

Fig. 13. Color distribution of the stars in the NGC 5128 field at different values of I. Part of the detections at $I < 23$ mag are due to AGB stars and Galactic foreground stars; about half of 111 (11) are simply due to photometric errors caused by the overlapping of two or more stars in our crowded field. The locus of the RGB in three globular clusters with different metallicities has also been displayed: the clusters are NGC 6752 ([Fe/H] = -1.54), NGC 1851 ([Fe/H] = -1.29) and 47 Tuc ([Fe/H] = -0.71).